Introducing Ambiguity Resolution in Web-hosted Global Multi-GNSS Precise Positioning with Trimble RTX-PP

Ken Doucet, Michael Herwig, Adrian Kipka, Philip Kreikenbohm, Herbert Landau, Rodrigo Leandro, Matthias Moessmer, Christian Pagels

Trimble TerraSat GmbH, Germany

ABSTRACT

In the middle of 2011 Trimble introduced the CenterPoint RTX real-time positioning service providing centimeter accurate positions for real-time applications. This service relies on the generation of precise orbit and clock information for GPS and GLONASS satellites in real-time. Support for the first Japanese QZSS satellite was recently added to the system. While existing PPP systems are available via web access today, the RTX-PP is unique with respect to the support of QZSS signals, the ability to resolve carrier phase ambiguities and the associated convergence performance.

The CenterPoint RTX service is providing real-time precise GNSS positioning for specific markets such as Precision Agriculture, Survey and Machine Control. The delivery of corrections for the receivers in the field occurs either via satellite link or internet connection.

This paper introduces the new Trimble RTX Post-Processing (RTX-PP) service which is running in the cloud providing absolute position estimates in the well-defined reference frame ITRF2008 using GPS, GLONASS and QZSS observations. The service is available as a web service as well as through a variety of Trimble office software products.

The achievable horizontal and vertical accuracy level of RTX-PP can be better than one centimeter with one day of measurement data. Since the convergence time of the solution is well below one hour, however, the delivered horizontal positioning accuracy is typically better than 2 centimeters after only one hour.

The paper presents the technology behind RTX-PP and discusses the different applications the service addresses. These include but are not limited to the establishment of precise reference frames with a well-defined datum; especially in areas without sufficient infrastructure, monitoring of the positions of GNSS reference stations for quality assurance purposes and tectonic motion and monitoring of deformation and subsidence.

Time series of position estimates will be presented to demonstrate the achievable accuracy in a variety of scenarios, including static and kinematic cases.

INTRODUCTION

For several years now Precise Point Positioning (PPP) solutions have been available via the Internet for GNSS users. These include the JPL APPS service based on Gipsy technology (Zumberge et al. 1997), the CSRS service of the Natural Resources of Canada (NRCAN9, (Mireault et al. 2008), the University of Brunswick service GAPS (Leandro et al. 2007), and the magicGNSS by GMV, Spain (Piriz et al. 2008). An overview and details on these services can be found in Wanninger et al. (2011).

The Trimble RTX-PP service introduces a number of unique features such as the processing of GPS, GLONASS and QZSS satellites and resolution of carrier phase integer ambiguities. It is based on a Trimble owned orbit and clock solution for the satellites which is derived from a global tracking network of more than 100 reference stations equipped with Trimble NetR5, NetR8 and NetR9 receivers. The global distribution of the network is shown in Figure 1.

The reference station receivers stream 1 Hz observation data to processing centers in the US and in Europe. At the processing centers the observations are used by multiple redundant servers to compute precise orbit and clock estimates which are then transmitted to users worldwide. In addition the servers store the parameter estimates in a compressed data format with 1Hz clock updates. This data is used as input for the RTX Post-Processing service.

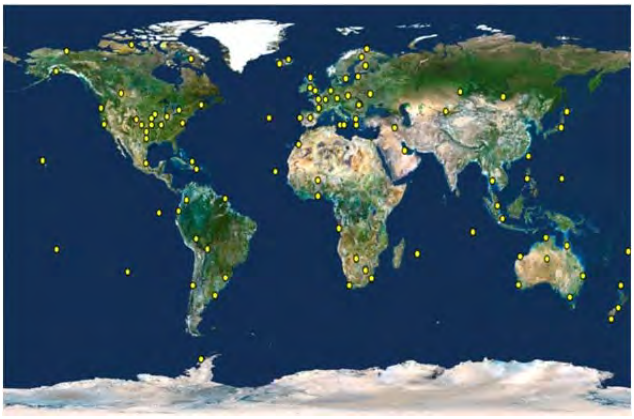

Figure 1: Trimble CenterPoint RTX tracking network

RTX-PP includes a free basic service plus a more advanced service which is restricted to Trimble software users only.

SERVER INFRASTRUCTURE SETUP

The RTX Post-Processing service (RTX-PP) is designed to serve a large number of users. The demands on the service with respect to availability and responsiveness are high. Since the number of clients is expected to increase rapidly there is also a strong focus on scalability without downtime. In order to fulfill these requirements the system was designed to run in the cloud.

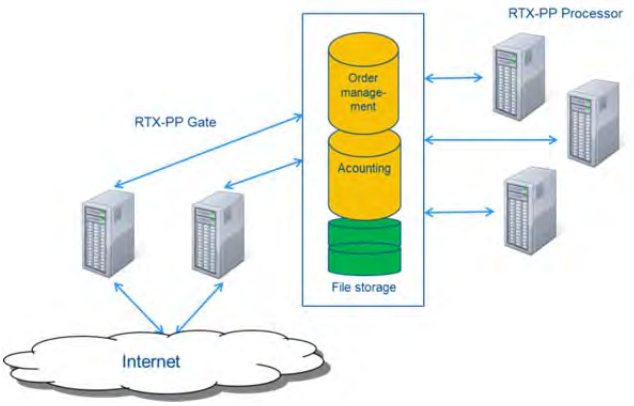

Figure 2: RTX-PP Server Infrastructure

As shown in Figure 2 the service consists of three parts; the communication interface, the processing engine and a database connecting the interface and engine. The database holds the files uploaded by clients, accounting information and the order management system.

The main purpose of the communication interface – RTX-PP Gate - is to retrieve orders, handle user accounting information and provide status information to the client. Each Gate module is able to handle multiple clients; having multiple instances of the Gate module will increase the bandwidth and decrease the risk of service unavailability. Typically two instances of the Gate module are run behind a load balancer. The user interface for the RTX-PP service is shown in Figure 3.

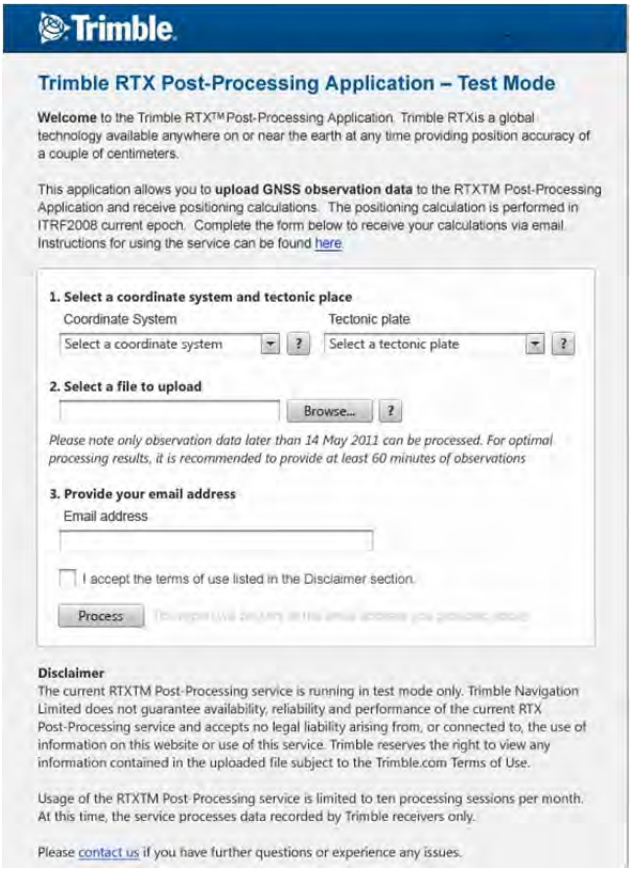

Figure 3: RTX-PP.COM web interface

The RTX-PP processing engines are independent from the Gate module; they search in the order management for the next available order, pick up the respective files and run the computation. During processing the engines update the order management with the current progress to be available to the client through the Gate. Each RTX-PP processor module runs multiple RTX-PP engine instances - typically one per hardware core – for best usage of computation power. The time an order stays in the system until the final result is sent to the client depends, of course, on the overall number of orders. To decrease the live time of the order additional RTX-PP processing modules would scale up the available computation power and thus will decrease the waiting time of the client. We run specialized clients in our environment to monitor the average time an order is in the system, if that is above a threshold we scale up with additional computation power.

Utilizing cloud technology ensures highest availability on a proven technology backbone. We can immediately react on load requirements to ensure maximum uptime with minimum response time.

PRECISE POSITIONING WITH RTX

RTX Post-Processing makes use of the precise orbits and clocks derived by the Real-time CenterPoint RTX System (Leandro et al. 2011). Orbit, clock and additional bias information is derived by the real-time server systems and stored in a compressed data format for use by the post-processing system. The underlying update rate of the satellite clocks is 1 Hz, i.e. allowing maximum accuracy and high update rates for kinematic rover positioning. Since the real-time server system is providing up to date information with minimum latency of less than one hour there is no significant delay in the possible processing of data with the web hosted RTX Post-Processing system.

The current system supports the processing of dual-frequency pseudorange and carrier phase observations of GPS, GLONASS, and QZSS satellites. It is based on the following fundamental measurement equations:

$$P_{i,k}^{j} = \left|r_i(t_i) - r^j\left(t_i - \tau_i^j\right)\right| + c \cdot \Delta t_i - c \cdot \Delta t^j + T_i^j + I_{P,i,k}^j + b_{P,i,k} - b_{P,k}^j + m_{P,i,k}^j + \epsilon_{P,i,k}^j$$

$$\Phi_{i,k}^{j} = \left|r_i(t_i) - r^j\left(t_i - \tau_i^j\right)\right| + c \cdot \Delta t_i - c \cdot \Delta t^j + T_i^j + I_{\Phi,i,k}^j + b_{\Phi,i,k} - b_{\Phi,k}^j + \lambda_k \cdot N_{i,k}^j + m_{\Phi,i,k}^j + \epsilon_{\Phi,i,k}^j$$

with

$r_i(t_i)$	Receiver position at time t_i
$r^j\left(t_i - \tau_i^j\right) = r^j\left(t^j\right)$	Satellite position at time of transmission t^j
$p_i^j = \left\|r_i(t_i) - r^j\left(t_i - \tau_i^j\right)\right\|$	Receiver to satellite range
c	Speed of light
Δt_i	Receiver clock error
Δt^j	Satellite clock error
T_i^j	Tropospheric delay
$I_{P,i,k}^j$	Ionospheric code delay in frequency *k*
$I_{\Phi,i,k}^j = -I_{P,i,k}^j$	Carrier phase advance due to ionosphere in frequency *k*
$b_{P,i,k}$	Receiver code bias
$b_{\Phi,i,k}$	Carrier phase receiver bias
$b_{P,k}^j$	Satellite code bias
$b_{\Phi,k}^j$	Satellite carrier phase bias
λ_k	Carrier wavelength of frequency *k*
$N_{i,k}^j$	Carrier phase integer ambiguity
$m_{P,i,k}^j$	Code multipath
$m_{\Phi,i,k}^j$	Carrier multipath
$\epsilon_{P,i,k}^j$	Code measurement error
$\epsilon_{\Phi,i,k}^j$	Carrier measurement error

The first order ionospheric effect in RTX positioning is eliminated via the "ionospheric free" combination of L1 and L2 frequencies and the troposphere is handled via a model plus additional unknowns for the vertical wet delay and two gradients in north-south and east-west direction. We estimate independent receiver clock errors for GPS and GLONASS while the QZSS satellite is assumed to have the same receiver clock error as GPS.

Corrections applied to the measurements are:

- Satellite and receiver antenna corrections
- Solid earth tides
- Pole tides
- Ocean tide loading effects
- Relativistic corrections
- Phase windup
- Code and carrier phase biases

The estimation is done via a UD filter implementation using the integer nature of the carrier phase ambiguities. The convergence of the ambiguities over time can be nicely seen in Figure 4. In the example shown the ambiguities converge to integer values after approximately 900 seconds.

SUPPORTED REFERENCE FRAMES

Since the CenterPoint RTX service provides satellite orbits in the ITRF2008 reference frame (current epoch) the receiver positions estimated by the RTX-PP engine are therefore also in ITRF2008 (current epoch. The user, however, may select a second frame to which they want

the position to be transformed. The reference frames that are currently supported are:

- ITRF 1988 to ITRF 2008
- NAD83, NAD83-CSRS, NAD83-CORS96, NAD83-2011, NAD83-MA11, NAD83-PA11
- ETRS89, ETRF2000-R05
- GDA94
- SIRGAS2000, SIRGAS95, SIRGAS-CON

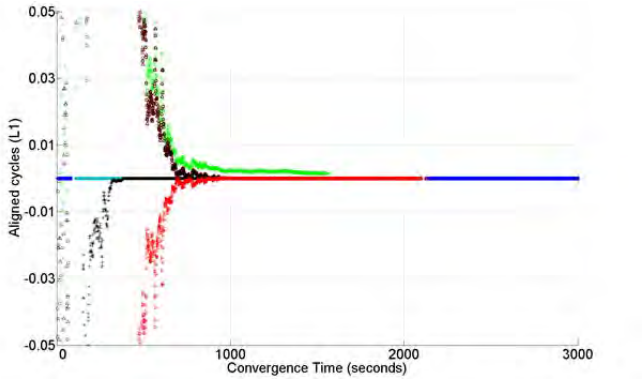

Figure 4: Typical GPS carrier phase ambiguity convergence plot

If individual station velocities are unknown and the user desires to determine a position on a specific tectonic plate the RTX-PP service allows transforming the ITRF2008 position to another frame with a different reference epoch and on a selected tectonic plate. The service uses plate rotations provided by Altamini (2007) and Bird (2003). The following tectonic plates are supported: Africa, Amurian, Antarctica, Arabia, Australia, Caribbean, Cocos, Eurasia, India, Juan de Fuca, Nazca, North America, Nubia, Okhotsk, Pacific, Philippine, Rivera, Scotia, South America, South Bismarck, Somalia, Yangtze.

RTX POST-PROCESSING

The RTX Post-Processing service is accessible via www.rtx-pp.com. This website provides a free service for static positioning of Trimble GNSS receivers. A complete list of the supported receivers and antennas can be found at that site. The files to be uploaded and processed can be in RINEX 2 and RINEX 3 data format and in Trimble proprietary data formats (e.g. DAT, T01, T02 files). The RTX-PP server does process data with up to 1 Hz update rate and requires files with at least one hour of data. Other restrictions for the free service are that the user cannot process more than 10 files per month and each file cannot span more than one day. The result of the processing is sent back to the user via email in PDF and XML format.

Kinematic processing is possible but reserved for use with Trimble infrastructure and office software, it is not available via the free web access. As an example, Trimble VRS infrastructure software, TPP 2.1 allows the processing of static and kinematic data for monitoring of reference station coordinates. Together with the real-time RTX processing in Trimble VRS³Net the post-processing of RTX is ideal for monitoring earth crustal motion, deformation and subsidence.

Static Positioning Performance

As stated previously the RTX-PP processing engine is typically able to fix carrier phase ambiguities to integer values 15 minutes after a cold start or a full engine reset. This greatly reduces the convergence time required to achieve a given level of accuracy.

Static position convergence with and without ambiguity fixing was investigated using data from a tracking station in Höhenkirchen, Germany, that was collected over a two week period. The station uses a rooftop mounted Trimble Zephyr Geodetic II antenna. The RTX-PP engine was run on the 14 days of data with and without ambiguity fixing and with full resets every hour. Horizontal and vertical position errors from all of the 336 hour runs were then used to determine the expected 68% and 95% positioning accuracy.

Horizontal position convergence curves and the corresponding statistical measures are shown in Figure 5. The vertical axis is the horizontal position error with a range of 0 to 0.1 meters while the horizontal axis is the convergence time with a range of 0 to 60 minutes. The cyan and blue time series are the 68% and 95% horizontal position errors with ambiguity fixing as a function of convergence time. Similarly, the red and pink time series are the 68% and 95% horizontal position errors without ambiguity fixing as a function of convergence time. These time series clearly demonstrate that we can achieve a given level of horizontal accuracy much more quickly with ambiguity fixing. In this example a horizontal accuracy of 3 centimeters (95%) is achieved about 3x faster with ambiguity fixing.

Vertical position convergence curves and the corresponding statistical measures are shown in Figure 6. Again, the time series clearly demonstrate that we can achieve a given level of vertical accuracy much more quickly with ambiguity fixing. In this example a vertical accuracy of 3 centimeters (95%) is achieved about 2x faster than it would be without ambiguity fixing.

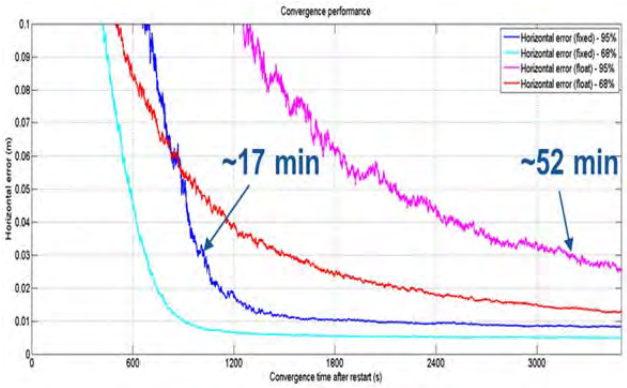

Figure 5 Fixed vs float horizontal convergence

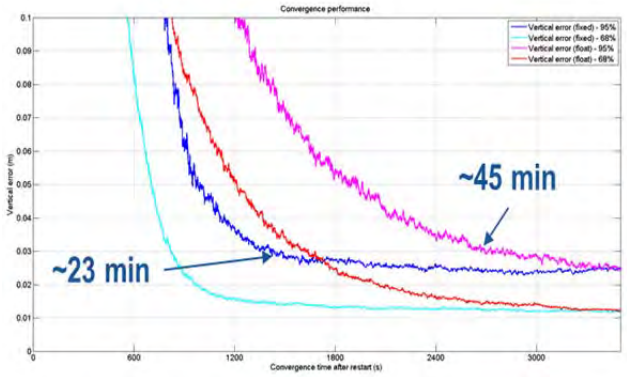

Figure 6 Fixed vs float vertical convergence

General static positioning convergence in the first hour was investigated by using data streams from 79 globally distributed monitoring stations with full resets of the RTX-PP engine every hour. The static convergence performance during the first hour after switching on the receiver was then analyzed for 16 days in spring 2012. The horizontal position convergence curves are shown in Figure 7. The vertical axis is the horizontal position error with a range of 0 to 0.1 meters while the horizontal axis is the convergence time with a range of 0 to 55 minutes. The green time series is the average horizontal position error as a function of convergence time. Similarly, the pink, cyan and red time series are the 68%, 90% and 95% horizontal position errors, respectively, as a function of convergence time. These time series demonstrate that 30 minutes after startup the horizontal position accuracy is expected to be approximately 1 centimeter on average or 2 centimeters 95% of the time.

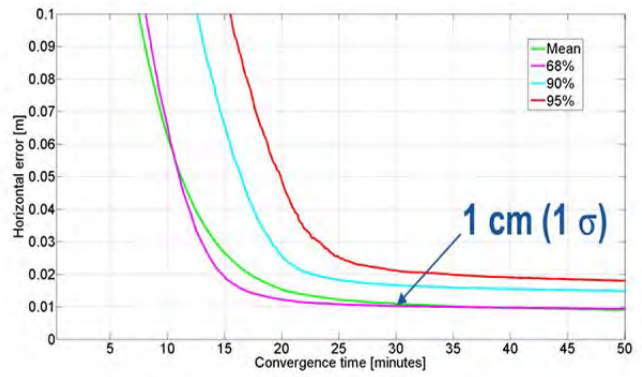

Figure 7: Static horizontal convergence

Similarly the mean, 68%, 90% and 95% vertical position convergence curves are shown in Figure 8. These time series demonstrate that 30 minutes after startup the vertical position accuracy is expected to be approximately 2.5 centimeters on average or 5 centimeters 95% of the time.

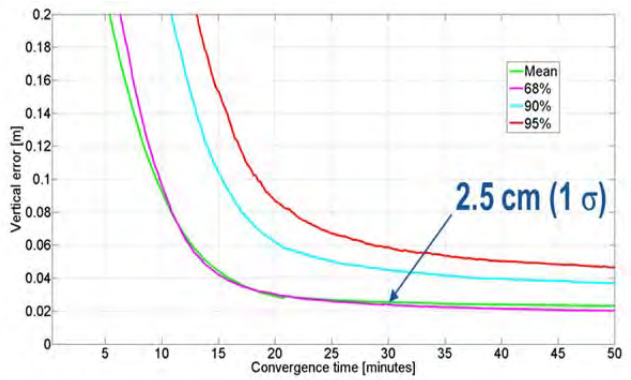

Figure 8: Static vertical convergence

To demonstrate the achievable position accuracy with different time spans the two weeks of data from the Höhenkirchen tracking station was reprocessed in ½, 1 hour, 2 hour, 3 hour, 4 hour, 6 hour, 12 hour and 24 hour segments. Time series of the north (blue), east (red) and height (green) errors for each segment are plotted in Figure 9 through Figure 16.

Table 1 summarizes the results obtained for each time period that was processed. As expected, the results show nicely the correlation between position accuracy and observation time. As the time period is increased the RMS values decrease but it also becomes obvious that the truth coordinates used for this station may be offset by a few millimeters. For the ½ hour time period a horizontal accuracy of 6.6 millimeters (1σ) was obtained surpassing the expected horizontal accuracy of 10 millimeters (1σ). For the same time period a vertical accuracy of 16.5 millimeters was obtained again surpassing the expected vertical accuracy of 25 millimeters (1σ).

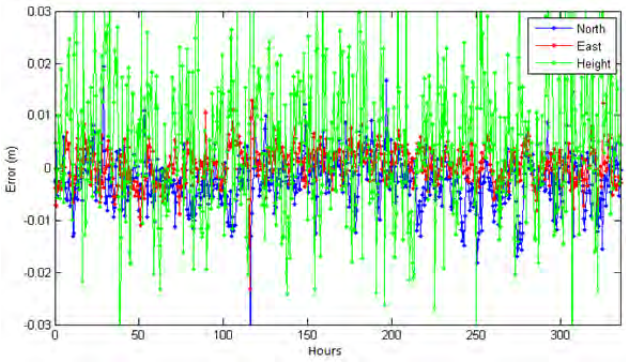

Figure 9 Position errors for 1/2 hour periods

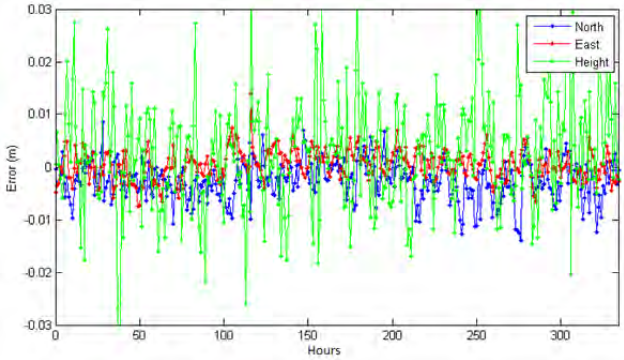

Figure 10 Position errors for 1 hour periods

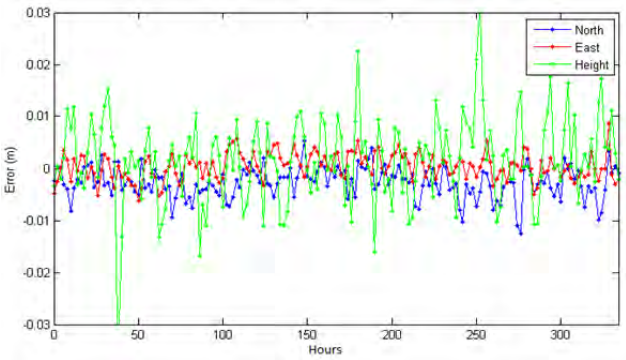

Figure 11 Position errors for 2 hour periods

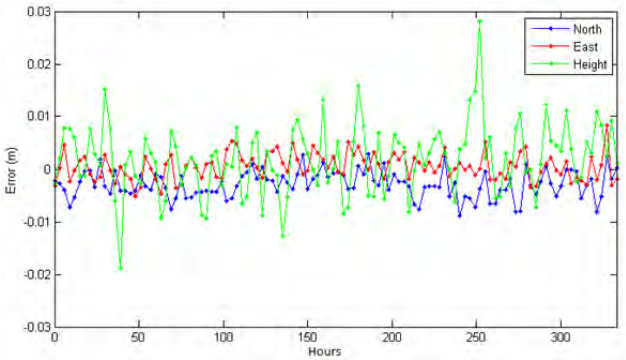

Figure 12 Position errors for 3 hour periods

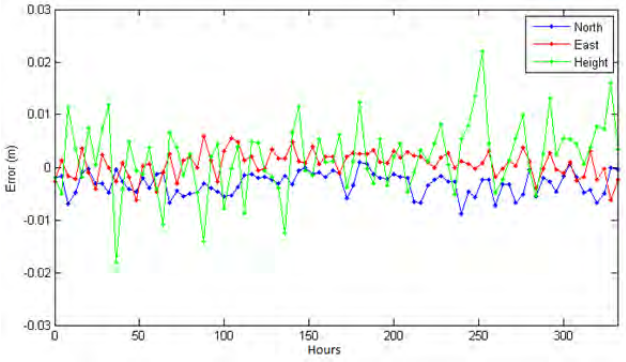

Figure 13 Position errors for 4 hour periods

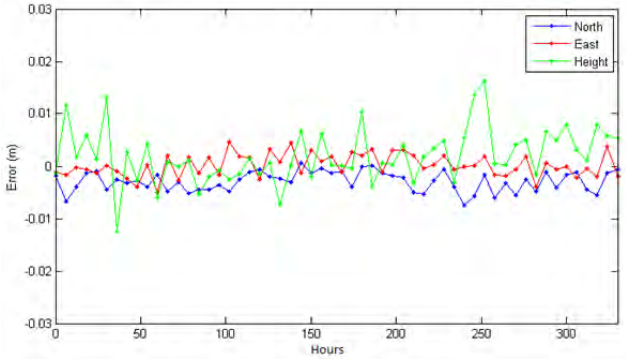

Figure 14 Position errors for 6 hour periods

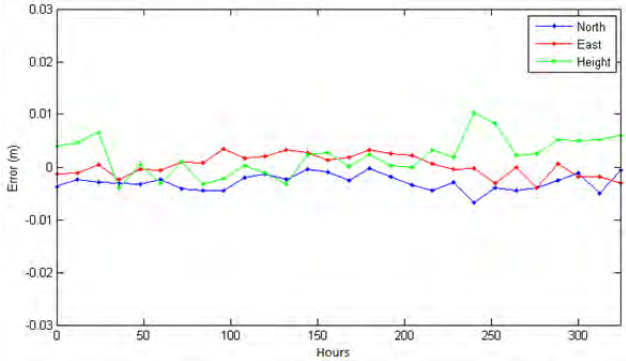

Figure 15 Position errors for 12 hour periods

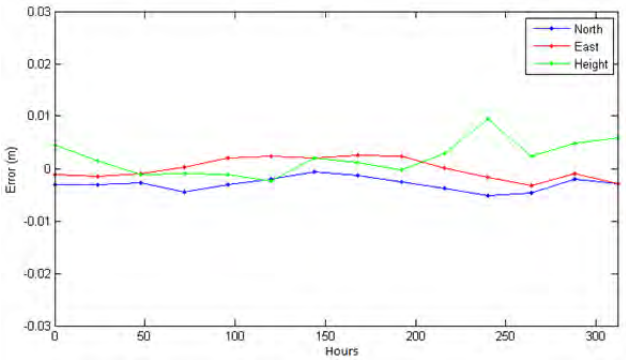

Figure 16 Position errors for 24 hour periods

Time period (hour)	Mean (mm)			RMS (mm)		
	North	East	Up	North	East	Up
0.5	-2.4	0.5	6.1	5.5	3.6	16.5
1	-2.6	0.5	3.0	4.5	2.9	11.5
2	-2.7	0.4	1.8	4.0	2.6	8.4
3	-2.9	0.5	2.0	3.9	2.6	7.0
4	-3.1	0.6	1.9	3.7	2.5	6.8
6	-2.9	0.2	2.0	3.5	2.2	5.6
12	-2.9	0.3	2.1	3.3	2.1	4.1
24	-3.0	0.0	2.0	3.2	2.0	3.7

Table 1: Mean position error and RMS for different time periods

To assess absolute accuracy daily measurement files from nine IGS stations collected between March 1st, 2012, and September 1st, 2012, were downloaded and post-processed using the RTX-PP service. The nine stations are shown in Figure 17.

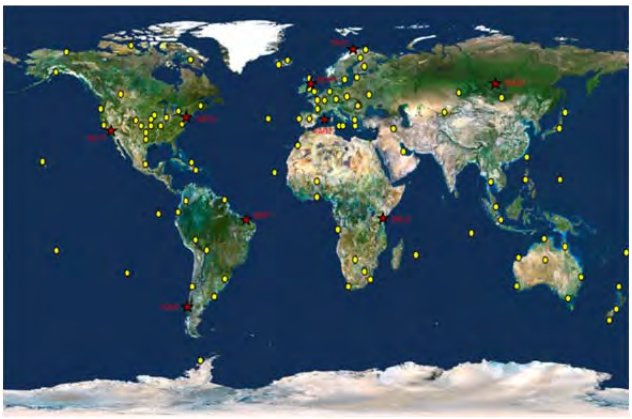

Figure 17 IGS stations

One of the criteria for choosing these stations is the mix of receivers and antenna from different GNSS equipment manufacturers. As shown in Table 2 the receivers used at these stations are manufactured by Javad Positioning Systems, Leica, Topcon Positioning Systems and Trimble while the antennas are manufactured by Ashtech, Allen Osbourne, Javad Positioning Systems, Leica and Trimble.

During the post-processing antenna phase center corrections for the satellite and receiver antennas were computed using the IGS ANTEX file for GPS week 1700. Each of the ~1656 daily RTX-PP solutions were compared to a truth position computed using the IGS08 epoch 2005.0 positions and velocities from the IGS week 1700 combined adjustment.

Code	IGS receiver name	IGS antenna name
BADG	JAVAD TRE_G3TH DELTA	JAVRINGANT_DM JVDM
BLYT	TRIMBLE NETRS	ASH701945B_M ENCL
BRFT	LEICA GRX1200PRO	LEIAT504
CAGZ	TPS E_GGD	JPSREGANT_DD_E NONE
CONZ	LEICA GRX1200+GNSS	LEIAR25.R3 LEIT
MAL2	JPS LEGACY	ASH701945C_M NONE
MORP	TRIMBLE NETR8	AOAD/M_T NONE
TRO1	TRIMBLE NETR8	TRM59800.00 SCIS
WES2	LEICA GRX1200GGPRO	AOAD/M_TA_NGS

Table 2 IGS station GNSS receivers and antennas

Figure 18 to Figure 21 show the north (blue), east (red) and height (green) offsets of the daily solutions over the six month period with respect to the IGS truth positions for four of the IGS stations that use receivers from the four manufacturers. In these plots the vertical axis is the position error with a range of ±3 centimeters while the horizontal axis is the number of days from March 1st, 2012, with a range of 0 to 184 days. Table 3 summarizes the results for all nine stations. In these results there are no obvious biases common to all stations and the overall accuracy of the RTX-PP daily solutions relative to IGS truth is about 6 millimeters horizontal (1σ) and 8 millimeters vertical (1σ).

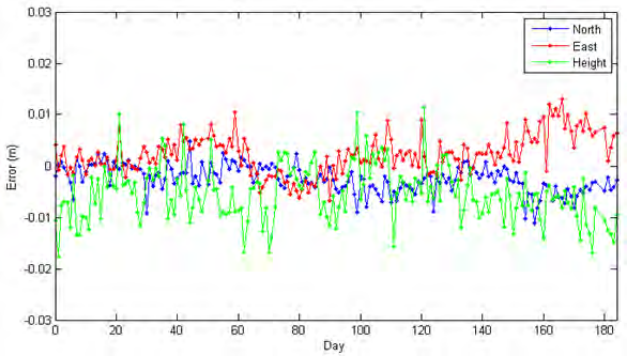

Figure 18 BADG (Javad) daily solutions position errors

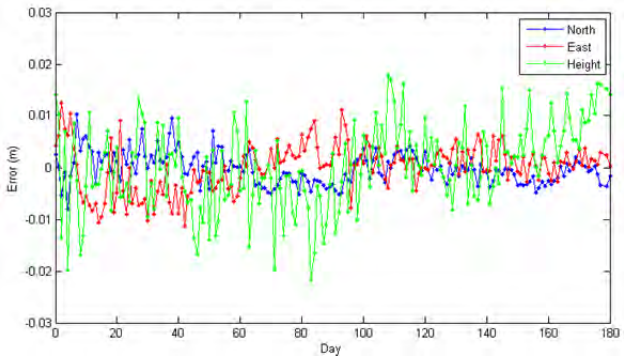

Figure 19 BRFT (Leica) daily solutions position errors

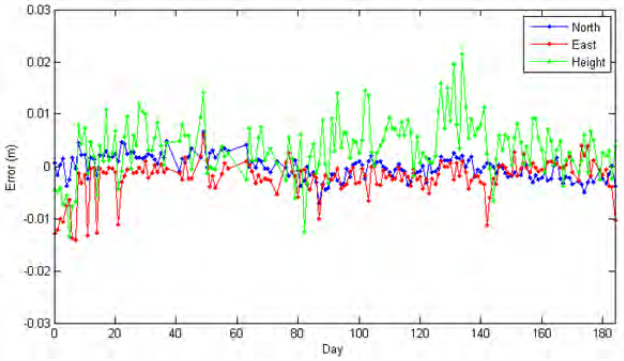

Figure 20 CAGZ (Topcon) daily solution position errors

Code	Mean (mm)			RMS (mm)		
	North	East	Up	North	East	Up
BADG	-2.5	2.3	-5.4	3.6	4.4	7.6
BLYT	-3.4	-0.2	-4.6	4.0	4.5	7.4
BRFT	-0.2	0.1	0.4	3.0	4.5	8.3
CAGZ	-0.2	-2.1	3.6	2.2	4.0	6.4
CONZ	-5.6	0.2	-4.7	7.4	5.8	9.1
MAL2	-3.0	-2.2	-1.0	4.6	6.3	7.6
MORP	3.1	-1.3	-6.0	3.7	3.5	7.5
TRO1	1.5	-0.3	2.5	2.8	2.4	6.5
WES2	-0.1	-2.4	-5.5	2.1	4.2	9.4
ALL				4.0	4.5	7.8

Table 3 IGS station 6 month daily solution summary

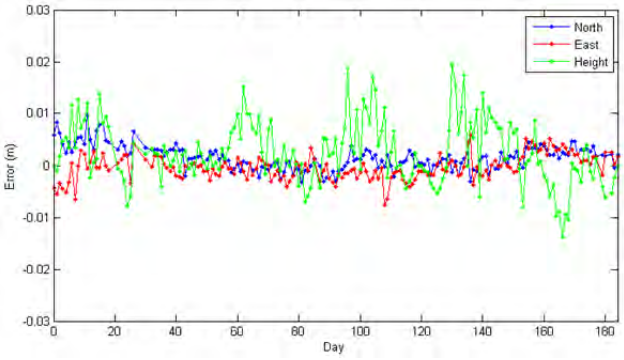

Figure 21 TRO1 (Trimble) daily solutions position errors

Kinematic Positioning Performance

To determine the expected kinematic positioning accuracy the previously discussed general convergence test was repeated but with the RTX-PP engine in kinematic mode. The horizontal position convergence curves for this test are shown in Figure 22. The vertical axis is the horizontal position error with a range of 0 to 0.1 meters while the horizontal axis is the convergence time with a range of 0 to 55 minutes. The green time series is the average horizontal position error as a function of convergence time. Similarly, the pink, cyan and red time series are the 68%, 90% and 95% horizontal position errors, respectively, as a function of convergence time. These time series demonstrate that 30 minutes after a cold start or a full reset of the processing engine the horizontal position accuracy is expected to be approximately 1.5 centimeters on average or 3.5 centimeters 95% of the time.

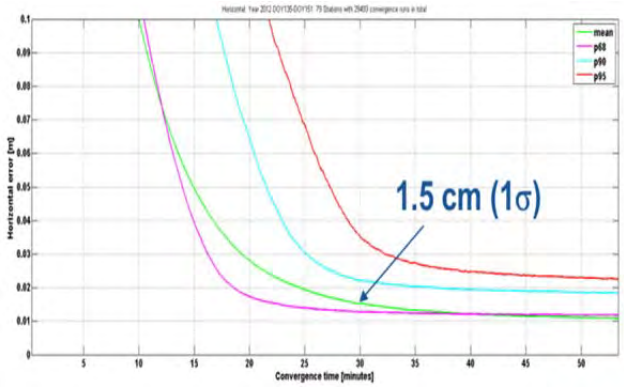

Figure 22 Kinematic horizontal position convergence

Similarly the mean, 68%, 90% and 95% vertical position convergence curves are shown in Figure 23. These time series demonstrate that 30 minutes after a cold start or a full reset of the processing engine the vertical position

accuracy is expected to be approximately 2.5 centimeters on average or 6.8 centimeters 95% of the time.

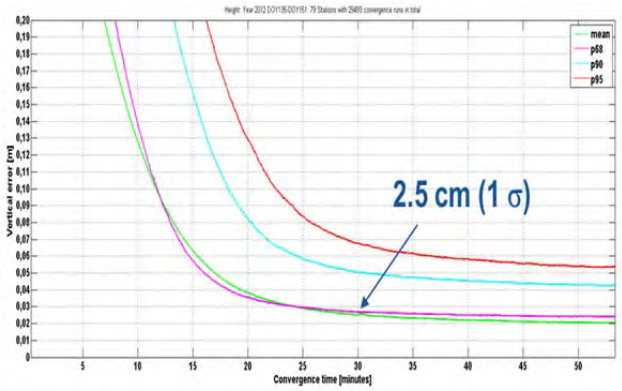

Figure 23 Kinematic vertical position convergence

Note that since the RTX-PP kinematic solution is post-processed - with multiple forward and backward passes - the horizontal and vertical position accuracy shown in Figure 22 and Figure 23 is available for the entire kinematic trajectory.

To demonstrate RTX-PP performance for kinematic applications GNSS measurements collected during an airborne survey and one land vehicle survey were post-processed using the RTX-PP service and the resulting positions compared to those obtained by conventional kinematic post-processing (KIN-PP) with Trimble Business Center (TBC) software.

The airborne data set was collected on December 23rd, 2011, in the Toronto area. The flight path is shown in Figure 24. During the flight the maximum velocity of the aircraft was 218 km/hour, the maximum distance from the base station was 134 kilometers and the maximum height difference relative to the base station was 1474 meters. The GNSS receiver used at the base station was a Trimble NETR5 and the antenna was a Trimble Zephyr Geodetic Model 2. The GNSS receiver used in the aircraft was a Trimble BD960 while the antenna was a Trimble Zephyr Geodetic.

Figure 25 shows the north, east and height differences between the RTX-PP and KIN-PP solutions. The vertical axis shows the position difference with a range of += 100 millimeters while the horizontal axis is time with a range of 0 to 240 minutes. The mean offsets between the RTX-PP solution and the KIN-PP solutions are -1.5, 5.7 and 10.1 millimeters in the north, east and height components, respectively, with corresponding RMS errors of 8.6, 10.3, and 23.5 millimeters. These results easily meet the expected 95% horizontal and vertical positioning accuracy of 3.5 centimeters and 6.8 centimeters, respectively.

Figure 24: Toronto flight path

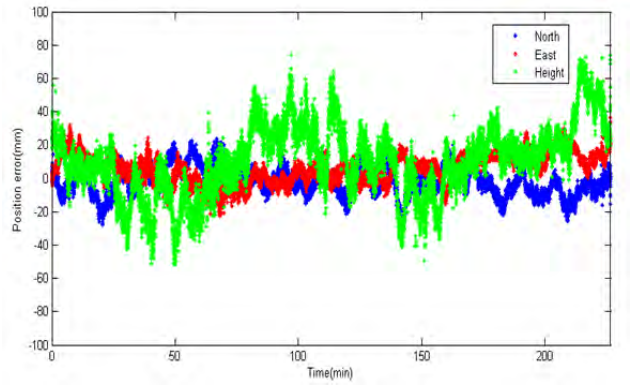

Figure 25: Toronto airborne test – RTX-PP vs KIN-PP

The land vehicle data set was collected on March 28th, 2012, in the Toronto area. The route for this survey is shown in Figure 26. During the drive the maximum velocity of the vehicle was 100 km/hour and the maximum distance from the base station was 3.3 kilometers. The GNSS receiver used at the base station was a Trimble NETR9 and the antenna was a Trimble Zephyr Geodetic Model 2. The GNSS receiver used in the van was a Trimble BD960 while the antenna was a Trimble Zephyr Geodetic.

Figure 27 shows the north, east and height differences between the RTX-PP and KIN-PP solutions. The mean offsets between the RTX-PP solution and the KIN-PP solutions are 4.7, -4.2 and 7.8 millimeters in the north, east and height components, respectively, with corresponding RMS errors of 11.9, 6.7, and 22.4 millimeters. As in the airborne case these results easily meet the expected 95% horizontal and vertical positioning accuracy of 3.5 centimeters and 6.8 centimeters, respectively.

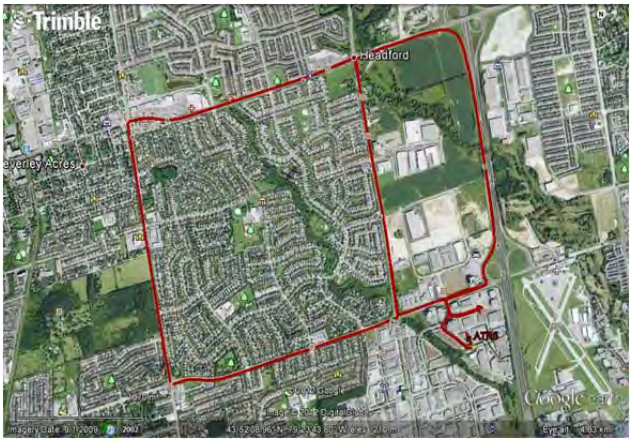

Figure 26: Toronto land vehicle test route

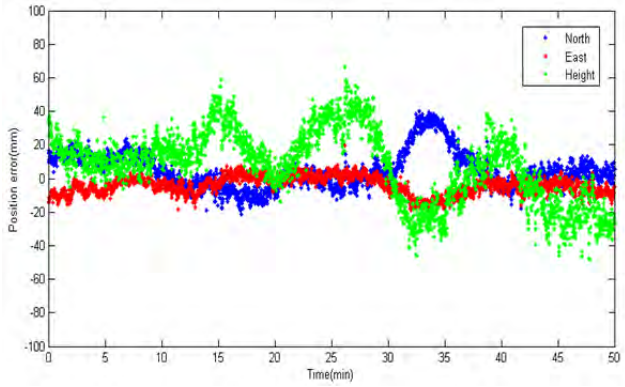

Figure 27: Toronto land test - RTX-PP vs KIN-PP

SUMMARY

The features that distinguish the RTX-PP service from other such services are multi-GNSS support (GPS, GLONASS and QZSS) and carrier phase ambiguity fixing in as little as 15 minutes after a cold start or a full reset of the processing engine. Because of these two features the RTX-PP service can be used to determine the absolute position of a GNSS antenna that is stationary for 30 minutes with a horizontal and vertical accuracy of 1 centimeter (1σ) and 2.5 centimeters (1σ), respectively. Of course the accuracy of the RTX-PP solution improves as the static occupation time is increased. With 24 hour static occupations we expect sub-centimeter (1σ) horizontal and vertical agreement with IGS truth.

For kinematic positioning the expected horizontal and vertical accuracy of the RTX-PP solution is 1.5 centimeters (1σ) and 2.5 centimeters (1σ), respectively, 30 minutes after a cold start or full reset of the processing engine. The RTX-PP kinematic solution is post-processed, however, so the horizontal and vertical position accuracy is therefore available for the entire kinematic trajectory.

REFERENCES

Altamimi et al (2007), *"ITRF2005: A new release of the International Terrestrial Reference Frame based on time series of station positions and Earth Orientation Parameters"*, Journal of Geophysical Research, Vol. 112, B09401, doi:10.1029/2007JB004949, 2007

Bird, P. (2003), *"An updated digital model of plate boundaries"*, Geochemistry, Geophysics, Geosystems and electronic journal of the earth sciences, Volume 4, Number 3, 14 March 2003, 1027, doi: 101029/2001GC000252, ISSN: 1525-2027

Giese, M., J. Kaczkowski, A. Lange, C. Stiegert, J. Wiegratz, P. Zakrzewski, L.Wanninger (2011) *„Post-Processing Services for Precise Point Positioning (PPP)“*, Allgemeine Vermessungsnachrichten Issue 3, 2011

Jaxa (2012) *Quasi-Zenith Satellite System Navigation Service Interface Specification for QZSS (IS-QZSS) version 1.4*, Japan Aerospace Exploration Agency February 28, 2012

Landau, H., M. Glocker, R. Leandro, M. Nitschke, R. Stolz, F. Zhang (2012) *„Aspects of using the QZSS Satellite in the Trimble CenterPoint™ RTX™ Service: QZSS Orbit and Clock Accuracy, RTX Positioning Performance Improvements”*, Paper presented at ION-GNSS-2012, September 17-21, 2012, Nashville, TN, USA

Leandro, R.F., Santos, M.C., Langley, R. B. (2007): GAPS: The GPS Analysis and Positioning Software – A Brief Overview. Proc. ION GNSS 2007, 1807-1811.

Leandro, R., H. Landau, M. Nitschke, M. Glocker, S. Seeger, X. Chen, A. Deking, M. Ben Tahar, F. Zhang, R. Stolz, N. Talbot, G. Lu, K. Ferguson, M. Brandl, V. Gomez Pantoja, A. Kipka, Trimble TerraSat GmbH, Germany (2011) *“RTX Positioning: the Next Generation of cm-accurate Real-time GNSS Positioning”*, Paper presented at ION-GNSS-2011, September 20-23, 2011, Portland, OR, USA

Mireault, Y., Tetreault, P., Lahaye, F., Heroux, P., Kouba, J. (2008): *"Online Precise Point Positioning"*. GPS World, Sept. 2008, pages 59-64.

Piriz, R., Mozo, A., Navarro, P., Rodriguez, D. (2008): "*magicGNSS: Precise GNSS products out of the box."* Proceedings ION GNSS 2008, 1242-1251.

Zumberge, J.F., Heflin, M.B., Jefferson, D. C.,Watkins, M.M., Webb, F. H. (1997): *"Precise Point Positioning for the efficient and robust analysis of GPS data from large networks"*. Journal of Geophysical Research, 102, B3:5005-5017.